Bulgarian Chemical Communications, Volume 46, Number 3 (pp. 585 – 593) 2014

Synthesis, characterization and properties of ZnO/TiO_2 powders obtained by combustion gel method

A. D. Bachvarova-Nedelcheva[1*], R. D. Gegova[1], A. M. Stoyanova[2], R. S. Iordanova[1],V. E. Copcia[3], N. K. Ivanova[2], I. Sandu[3]

[1]*Institute of General and Inorganic Chemistry, Bulgarian Academy of Sciences, Sofia, Bulgaria*
[2] *Medical University, Pleven, Bulgaria*
[3] *Arheoinvest interdisciplinary platform, Laboratory of the Scientific Investigation, Iasi*

Received July 4, 2013; Accepted November 28, 2013

Submicron ZnO/TiO_2 powders were obtained via combustion gel method. The structure, morphology and elemental composition of the obtained samples were characterized by XRD, IR spectroscopy and SEM with EDX analysis. The photocatalytic activities of the samples were evaluated by the degradation of Malachite Green and Reactive Black5 in aqueous solutions under ultraviolet light irradiation. The antibacterial properties of samples obtained via combustion sol-gel method were studied in solid media (agar plates) against Gram-negative Escherichia coli ATCC 25922 and Gram-positive Staphylococcus aureus ATCC 25923. The inhibition diameter was measured for all investigated samples. No clear zone of inhibition was seen around of blank experiments. Thus, all samples exhibited strong bactericidal action toward both selected bacterial cells.

Keywords: composite powders, sol-gel chemistry.

INTRODUCTION

Recently, the combustion synthesis (CS) became more popular and has emerged as an important technique for the synthesis and processing of oxide and non-oxide advanced materials [1]. This method has many potential advantages, such as low-processing cost, energy efficiency, and high production rate. Several books [2 - 4] and review articles [5 - 12] have been published on this subject in recent years. By combustion synthesis, TiO_2, nanoparticles sized from 100 nm to 1000 nm were very quickly obtained through gasification, nucleation, and crystal growth [13, 14]. Zinc oxide (ZnO) powders with different types of morphology were synthesized by a combustion synthesis method using zinc nitrate, metallic zinc and glycine as precursors [15]. Nanosized ZnO powder was synthesized by solution combustion method. The obtained powder showed three times higher photocatalytic efficiency than any other commercial photocatalysts [16]. Zn doped TiO_2 and N-doped TiO_2/ZnO composite powders were obtained by combustion method with better photocatalytic activity compared to pure TiO_2 [17]. Their photocatalytic properties were studied towards methyl orange dye. The authors reported that the enhanced photocatalytic activity of the composites is related to the good crystallization, the presence of anatase phase, and the particle size reduction.

It is well known that ZnO and TiO_2 oxides are close to being two of the ideal photocatalysts in several respects. In recent years, they become more attractive and important since it has a great potential for contribution to environmental problems. Several authors [18-19] found that the coupling of TiO_2 with ZnO is useful to achieving higher photocatalytic reaction rate. The results showed that the photocatalytic activity of ZnO/TiO_2 coupled photocatalysts was higher than that of the single phase. Although ZnO and TiO_2 in general have been proved to be very active in the photocatalytic oxidation of different pollutants, the problem concerning the influence of particles size and morphology on their performance efficiency is very crucial and not yet clarified. Both TiO_2 and ZnO were extensively studied as antimicrobial agents mainly under UV light irradiation [20-26]. It was found that TiO_2 is very effective in killing *Escherichia coli* (*E. coli*) [20], while ZnO is most effective in disinfection of *Staphylococcus aureus* (*S. aureus*) [24].

The present study is a continuation of our previous investigations in the $ZnO-TiO_2$ system. By applying different sol-gel methods we proved that the type of precursor and the order of adding the components influence on the microstructure of the

* To whom all correspondence should be sent:
E-mail: albenadb@svr.igic.bas.bg

final product. We also found that the selection of an appropriate scheme for synthesis is very important point [27]. Synthesis and antibacterial properties of nanosized powders obtained by aqueous and non-aqueous sol-gel methods in this system were studied recently by our team [28, 29]. Regardless of the large number of investigations in this system, studies of photocatalytic and antibacterial properties of ZnO/TiO_2 composite powders obtained via combustion method are very scarce.

The aim of the present study is to synthesize, characterize as well as to evaluate the photocatalytic and antibacterial properties of selected powder samples obtained by combustion gel method. The photocatalytic activity of obtained powders was verified toward Malachite Green (MG) and Reactive Black 5 (RB 5). The antibacterial activity was performed in solid media (agar nutritive) against the cells of *E. coli* and *S. aureus*.

EXPERIMENTAL

Samples preparation

Based on the results of our previous studies in this system [27, 30-32], samples with different nominal compositions $90ZnO.10TiO_2$ (sample A), $10ZnO.90TiO_2$ (sample B) and $5ZnO.95TiO_2$ (sample C) were selected for investigation (Table 1).

Table 1. Samples obtained by combustion gel method

samples N	*Nominal composition*	*Precursors*	*Final product according to X-ray diffraction*
A	$90ZnO.10TiO_2$.	Ti etoxide (sol A) + Zn nitrate (sol B)	ZnO
B	$10ZnO.90TiO_2$.	Ti etoxide (sol A) + Zn nitrate (sol B)	TiO_2 (rutile, anatase) + $ZnTiO_3$
C	$5ZnO.95TiO_2$.	Ti butoxide (sol A) + Zn nitrate (sol B)	TiO_2 (anatase)

The starting materials were: zinc nitrate – $Zn(NO_3)_2.6H_2O$ (Merck), titanium (IV) ethoxide (Fluka AG) - $Ti(OC_2H_5)_4$, titanium (IV) butoxide (Sigma-Aldrich) - $Ti(OC_4H_9)_4$ and ethylene glycol ($C_2H_6O_2$) (Table 1). The main scheme for the synthesis is presented in Fig. 1.

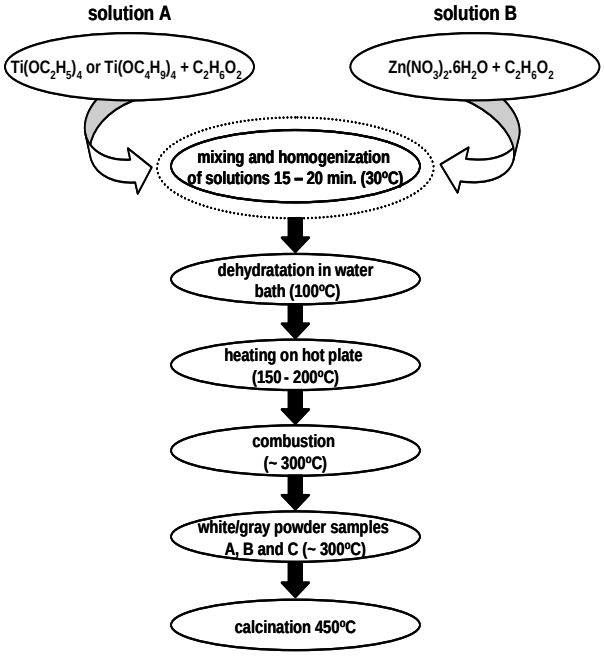

Fig. 1. Scheme for combustion gel synthesis of ZnO/TiO_2 powders

All solutions were prepared via dissolving of the precursors in ethylene glycol and absolute alcohol by means of vigorous magnetic stirring. A white xerogel was obtained by drying at 110°C for 5h. Subsequently, the as-obtained xerogel was subjected to evaporation in a water bath. During the heating on a hot plate up to 200-300°C, combustion process takes place and as a result gray-white powders were obtained. According to the classification for the combustion synthesis made by [1], our method could be classified as a gel combustion method. The last step of synthesis consists of calcinations of the powders at 400-450°C for 2 hours in air, until obtaining white powders (samples A, B and C). The calcinations temperature was selected on the basis of our previous investigations: from one side because there is almost no presence of organic constituents above 400^0C and from another - to keep the small size of the obtained crystals. All samples were prepared by addition of Ti precursor solutions to the zinc nitrate. During the experiments the measured pH varied from 5 to 7 depending on compositions.

Samples characterization

The phase formation and morphology of the obtained powders were established by X-ray diffraction (Bruker D8 Advance X-ray apparatus) and SEM (JEOL Superprobe 733). Scanning electron micrographs were obtained from a VEGA 11 LSH scanning electron microscope (TESCAN, Czech Republic). Samples were deposited on a sample holder with an adhesive carbon foil. The energy dispersive X-ray spectra-EDX patterns were carried out using a Quantax QX2 system (Bruker/Roentec, Germany). The main short range

orders of the obtained powders were determined by IR spectroscopy using the KBr pellets method (Nicolet-320, FTIR spectrometer with a resolution of $\pm 1 cm^{-1}$, by collecting 64 scans in the range 4000–400 cm^{-1}).

Photocatalytic activity experiments

The photocatalytic activities of the synthesized powders were evaluated by UV-light induced photobleaching of two model pollutants - Malachite Green (MG) and Reactive Black 5 (RB5) aqueous solutions. The initial concentrations of MG and RB5 solutions were 5 ppm and 11 ppm, respectively. The composite sample (100 mg) was added to 150 ml dye solution to form slurry. After that, the suspension was magnetically stirred in the dark for 30 min to ensure the establishment of an adsorption-desorption equilibrium. The irradiation source was a black light blue UV-lamp (Sylvania BLB 50 Hz 8W T5) with the major fraction of irradiation occurring at 365 nm. The lamp was fixed 10 cm above the solution surface. All photocatalytic tests were performed at constant stirring (400 rpm) and room temperature of 25ºC. At regular time intervals of illumination, aliquot samples of mixtures (3 mL) were collected and centrifuged in order to remove the solid particles. The discoloration was monitoring by measuring the absorbance of clear aliquots using Jenway 6505 UV-Vis spectrophotometer at maximum absorption wavelengths - 618 nm for MG and 600 nm for RB5.

Antibacterial measurements

Procedure for qualitative determination of inhibition zone

The strains of microorganisms - *E. coli* ATCC 25922 and *S. aureus* ATCC 25923, were cultured aerobically at 37ºC for 18 h in 10mL nutrient broth. 20 ± 2mL of sterilized nutrient agar (solid media) was dispersed into each standard flat bottom Petri dish to obtain firmly solid agar before inoculating. 2 mL of inoculum from the ten times diluted inoculum cultured was transferred on the surface of the sterile agar area of a Petri dish. After that the tested samples were gently pressed to contact intimately the agar surface and the inoculum. The obtained mixtures were incubated at 37ºC for 24 hours. The antibacterial activity is evident when a clear zone of inhibition of bacterial growth around the tested samples becomes visible.

RESULTS AND DISCUSSION

The X-ray diffraction patterns of obtained ZnO/TiO_2 white coloured powders are shown in Figure 2.

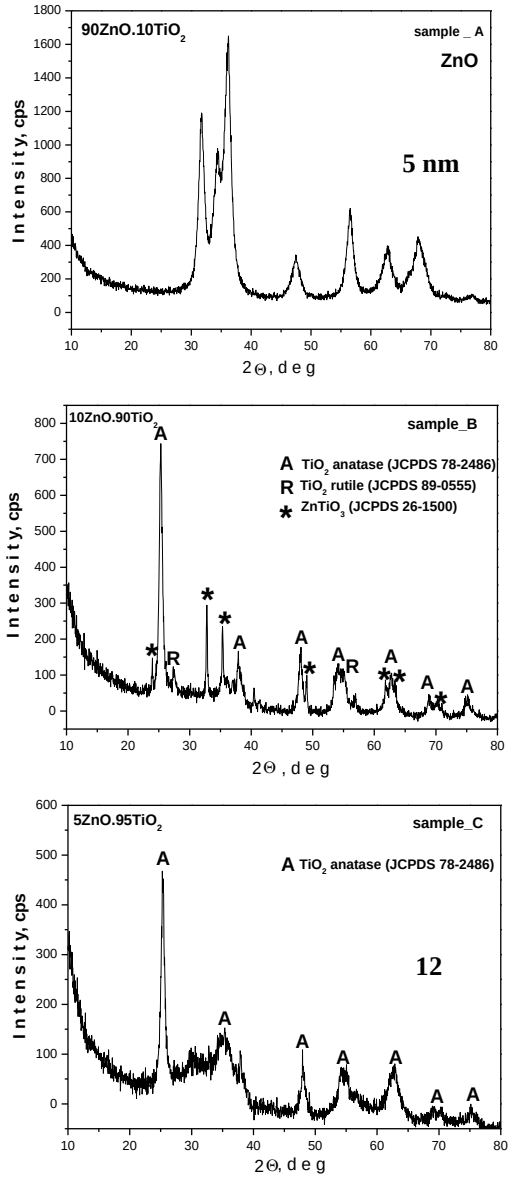

Fig. 2. XRD patterns of the investigated samples A, B and C

As can be seen different products were obtained. The characteristic peaks for zinc oxide (ZnO - JCPDS 36-1451) were identified in sample A. A mixture of TiO_2 polymorphous modifications (anatase - JCPDS 78-2486 and rutile - JCPDS 89-0555) as well as $ZnTiO_3$ (JCPDS 26-1500) were found is sample B, while anatase only, was separated in sample C. The average crystallite size of samples A and C calculated from the broadening of the diffraction line using Sherrer's equation are 5 and 12 nm, respectively. Our XRD results are compatible with the our previous data [33] as well as to the data reported for ZnO obtained by solution combustion method, where the size of the powders was found to be about 30 nm [16]. The SEM images and EDX spectra of obtained samples are presented in Fig. 3a, b, c.

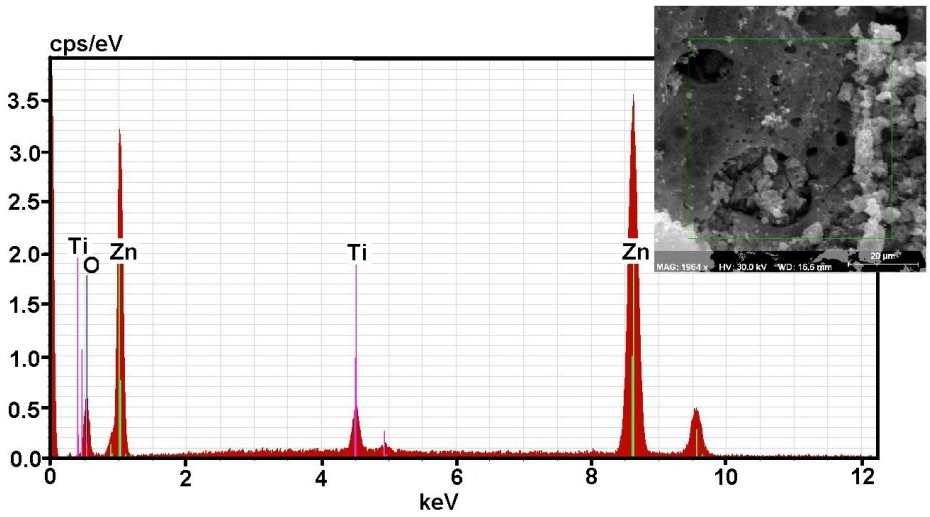

Fig. 3a. SEM micrograph and EDX spectrum of sample A

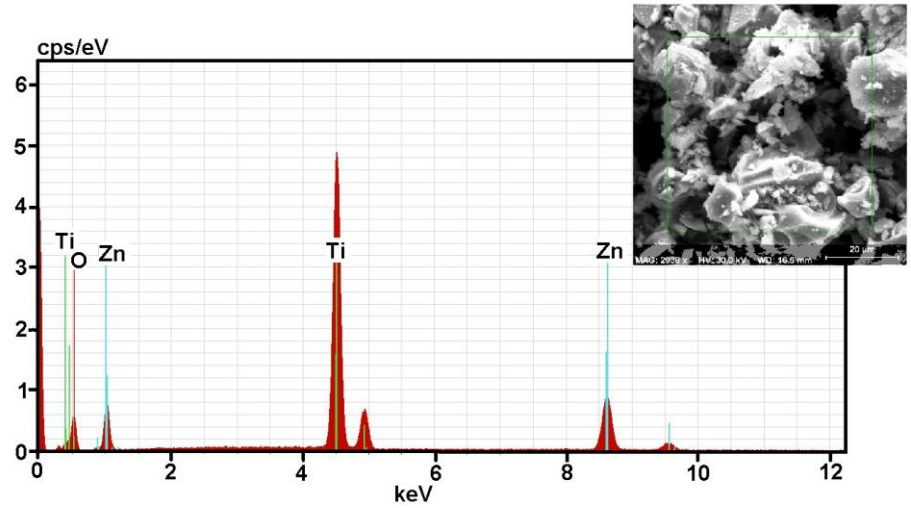

Fig. 3b. SEM micrograph and EDX spectrum of sample B

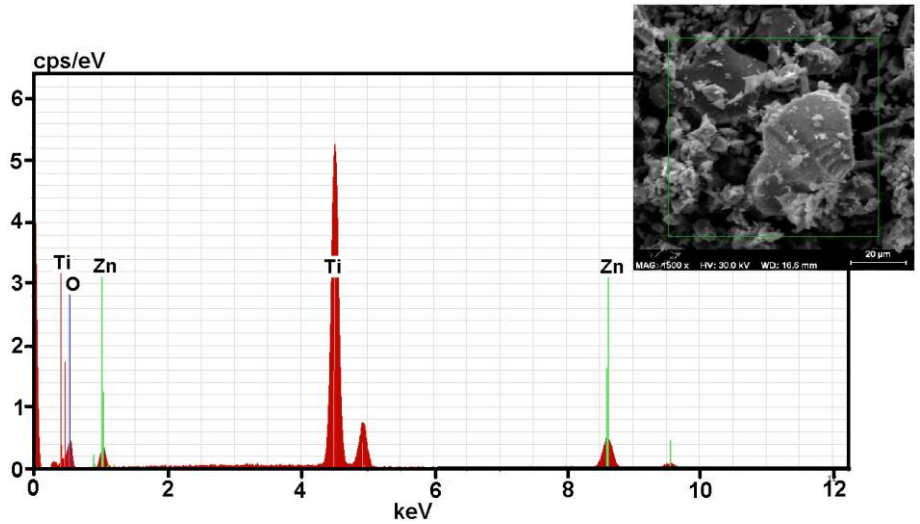

Fig. 3c. SEM micrograph and EDX spectrum of sample C

Irrespective that all samples are obtained by combustion method, the crystal morphology is different and sample A showed a porous agglomerate structure compared to the other two samples. The reason for that is may be due to the higher amount of zinc nitrate used as a precursor for ZnO at obtaining of this sample. This fact did not confirmed the previous suggestions of other

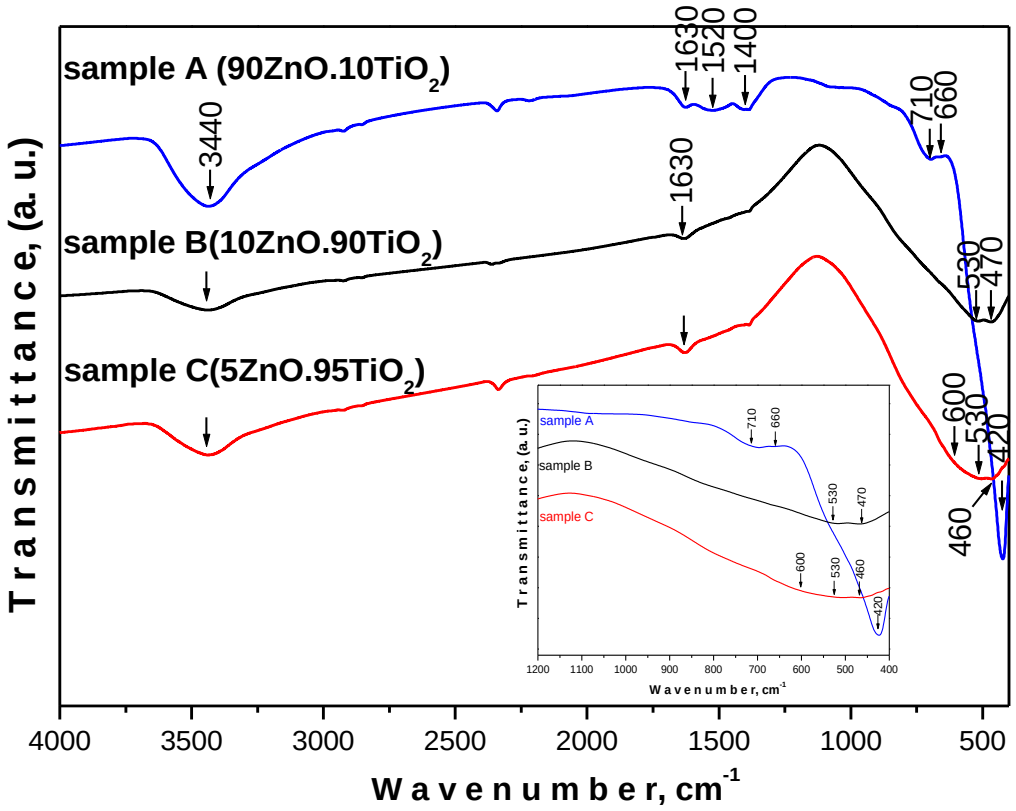

Fig. 4. IR spectra of the samples A, B and C in the range 4000 - 400 cm-1. The inset shows the IR spectra in the range 1200 - 400 cm-1.

authors, who claimed that Zn acetate leads to obtaining of more porous samples [18].

According to SEM observations (Figure 3a, b, c), during the calcinations, samples B and C are characterized by a strong tendency to agglomeration with the average particle size of the aggregates about 20-25 nm. The EDX results shows that the Ti, Zn and O are the principal components of investigated samples.

The IR spectroscopy was used in order to obtain an additional information for the phase formation in the investigated system. IR spectra of the powders calcinated at 450^0C are shown in Figure 4 and vibrations of the inorganic building units, only were recognized.In the spectrum of sample A ($90ZnO.10TiO_2$), dominant bands at 420 cm^{-1} along with weak shoulders at 700 and 660 cm^{-1} are observed. It is well known that bands in the absorption range 440-420 cm^{-1} could be related to the vibrations of ZnO_4 polyhedra [31, 34, 35]. The IR spectra of other two samples (B - $10ZnO.90TiO_2$ and C - $5ZnO.95TiO_2$) exhibited broad absorption region from 600 to 400 cm^{-1} in which follow the characteristic vibrations of ZnO and TiO_2 (anatase and rutile) [36, 37, 38]. The XRD patterns of the samples did not detected the presence of TiO_2 and ZnO, when they are in low content (5, 10 mol %). Despite that fact, their presence was registered by IR (weak bands at 700, 660 cm^{-1} and bands in the range 600-400 cm^{-1}) due to the higher sensibility of this method [37]. The observed at 3440 and 1630 cm^{-1} bands in all IR spectra may be assigned to the absorbed water molecule [37].

Photocatalytic activity

The changes in MG and RB5 dyes concentration C/C_o (C_o initial concentration and C reaction concentration of the dye) by the synthesized composite samples with the time of radiation are shown in Figure 5 a, b.

The kinetics of photocatalytic degradation of many organic compounds has often been modeled by the Langmuir-Hinshelwood treatment of heterogeneous catalytic systems [39-41], expressed by Eq. (1):

$$r = -\frac{dC}{dt} = \frac{k_r KC}{1+KC} \qquad (1)$$

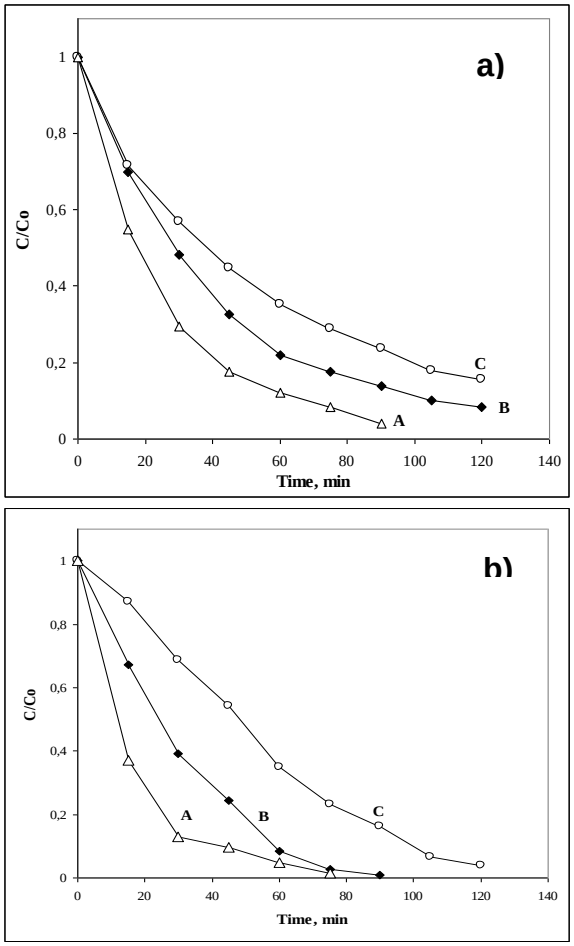

Fig. 5. Photocatalytic activity of samples A, B and C toward: a) MG and b) RB5.

where r represents the initial rate of photodegradation, i.e. dC/dt is the rate of disappearance of the pollutant, C is its concentration, k_r is the Langmuir-Hinshelwood reaction rate constant, and K is the Langmuir adsorption equilibrium constant. At a dilute concentration of pollutants ($C<10^{-3}$ M, i.e., $KC<<1$), pseudo-first-order kinetics model can be assumed as shown in Eq. (2):

$$-\frac{dC}{dt} = k_r K C \qquad (2)$$

Equation (2) can be integrated to expression (3):

$$ln\frac{C_o}{C} = k_r K t = k' t \qquad (3)$$

where C_o and C are, respectively, the initial concentration and the reaction concentration of the pollutant at time t, and k' – the apparent pseudo-first order rate constant. Under the same conditions, the initial degradation rate could be written in a form conforming to the apparent first order rate law:

$$r = k'C$$

The reaction kinetics for the initial 45 min of dyes degradation was studied by applying the pseudo-first order model expressed by equation (3). Figure 6 shows the plots of $ln(C_o/C)$ versus time for the studied samples. A good correlation to the pseudo-first order kinetics ($R>0.99$) was found from these results (Figure 6 a, b).

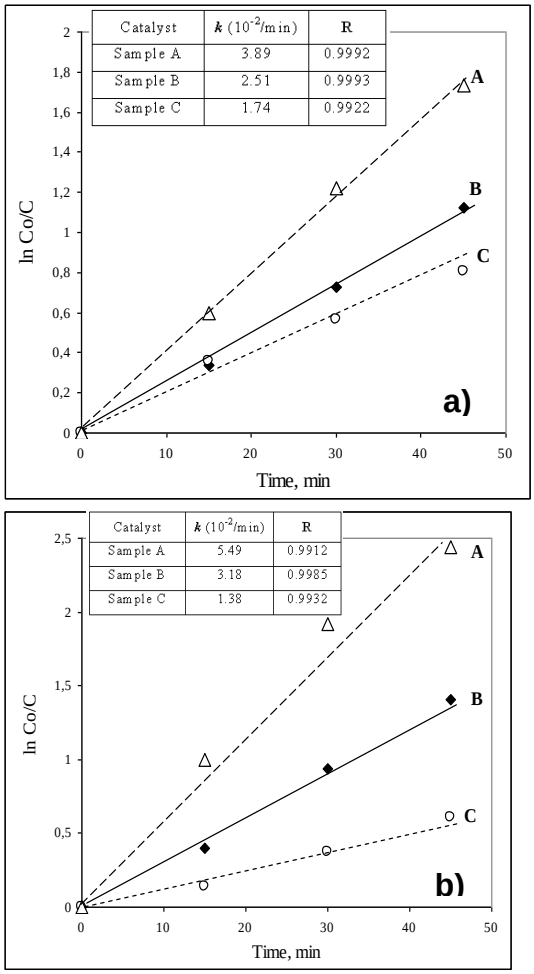

Fig. 6. Photocatalytic reaction kinetics of: a) MG decoloration and b) RB5 decoloration, both under UV irradiation.

The resulting first order rate constants were used for a comparison of the efficiency of photocatalytic process. The values of apparent rate constants show the highest photocatalytic activity of sample A on decoloration of both MG and RB5 dyes.

On one hand, the comparison between our present and previous results showed that as obtained ZnO/TiO_2 composite powders exhibited lower photocatalytic activity to that of pure ZnO and pure TiO_2 (~ 30 min toward MG and RB 5) under UV irradiation. On the other hand, the obtained results are better than those reported for TiO_2/ZnO composite powders obtained by combustion method, for which decolouration of azo dyes completed in 3 h under UV irradiation [42].

Antibacterial activity

The antibacterial activity was investigated by exposing studied microorganisms in nutritive media to the action of samples A, B and C. Each of the circular specimens with 5 mm diameter (filter paper with 0.005 g sample) was gently pressed on the *E. coli* and *S. aureus* inoculated agar surface before incubation. After incubation at 37°C for 24 h bacteria inhibition took place and a zone of inhibition appeared around the samples. No clear zone of inhibition was seen around the blank sample. The inhibition diameter was measured for all tested samples. The antibacterial activities of the samples against *E. coli* and *S. aureus* are presented in Fig. 7a and Fig. 7b, respectively.

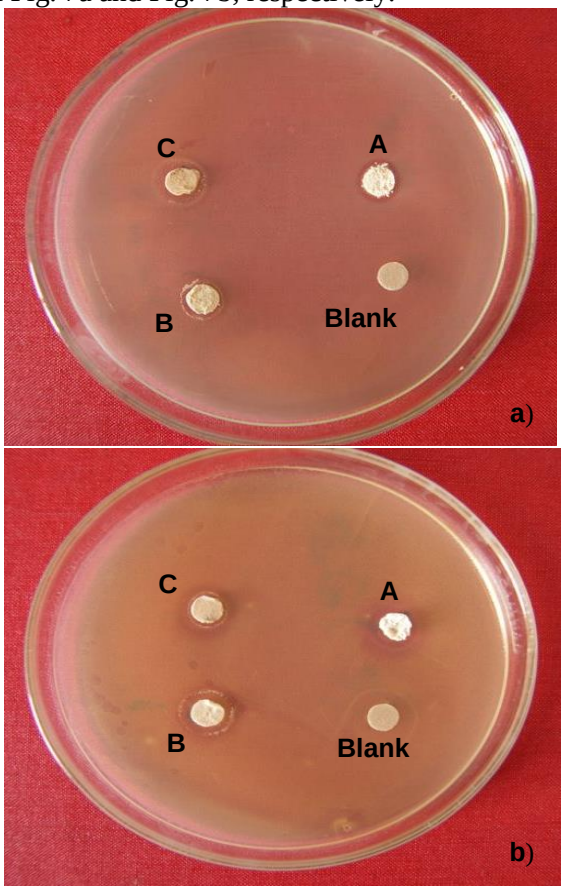

Fig. 7. Growth inhibition of the investigated samples for *E. coli* (a) and *S. Aureus* (b)

The antibacterial activity assessment of the powders is presented graphically in Figure 8. The synthesized ZnO/TiO_2 powders were found to have inhibition activity against both *E. coli* and *S. aureus*. The results for inhibition diameters are

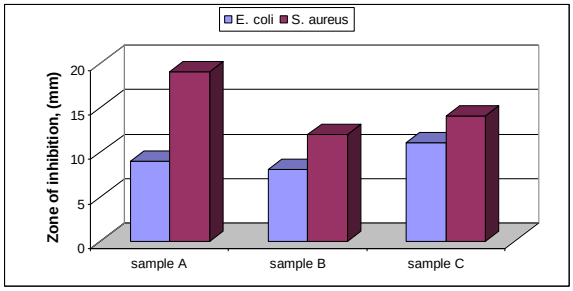

Fig. 8. Antibacterial activity assessment of the investigated samples for E. coli and S. Aureus

shown in Table 2. As can be seen, sample A exhibited the best antibacterial activity in disinfection of *S. aureus*, while sample C exhibited best results for *E. coli* disinfection. This can be explained probably by the sample composition. The results obtained are in accordance with our previous findings [27, 43] and to the results obtained by other authors. ZnO has been found to be more effective toward Gram- negative than to gram-positive bacteria and to exhibit a sustainable antibacterial activity even in the dark conditions [44 - 46]. As is shown in Table 2, sample A contains mainly ZnO, in sample B a mixture of anatase, rutile and $ZnTiO_3$ was found while sample C contains only anatase. It is known that the photocatalytic activity of pure rutile phase is lower than that of pure anatase phase [47, 48]. Probably, the reason for the reduced antibacterial efficiency of sample B is the presence of small amount of rutile in its composition.

CONCLUSIONS

Nanosized (5-12 nm) ZnO/TiO_2 powders were obtained via combustion gel method. The as-prepared powders exhibited good photocatalytic activity towards two organic dyes Malachite green and Reactive Black5 under UV light. The synthesized powders showed antibacterial activity against *E. coli* and *S. Aureus* without induction of irradiation. The antibacterial effect of sample rich in ZnO was more pronounced for the culture of *S. aureus* while the antibacterial effect of sample rich in TiO_2 (anatase) was stronger for the culture of *E coli*. The obtained powders could be a candidate for environmental and biomedical application after further investigations on their antimicrobial activity.

Table 2. Antibacterial activity of investigated samples

Samples	*Inhibition diameter (E. coli)*	*Inhibition diameter (S. aureus)*
A (ZnO)	9 mm	19 mm
B (A, R, $ZnTiO_3$)	8 mm	12 mm
C (TiO_2 - A)	11 mm	14 mm

REFERENCES

1. K. C. Patil, S. T. Aruna, S. Ekambaram, *Curr. Opin. Solid State Mater. Sci.*, **2**, 158 (1997).
2. A. G. Merzhanov, A. S. Mukasyan, *Combustion of solid flame*, Moscow: Torus Press; 336 (2007).
3. A. S. Mukasyan, K. Martirosyan, editors, *Combustion of heterogeneous systems: fundamentals and applications for material synthesis*. Kerala, India: Transworld Research Network, 234 (2007).
4. A. A. Borisov, L. De Luca, A. G. Merzhanov, editors, *Self-propagating high temperature synthesis of materials*, New York: Taylor and Francis, p. 337 (2002).
5. A. M. Segadaes, *Eur. Ceram. News Lett.*, **9**, 1 (2006).
6. A. Varma, V. Diakov, E. Shafirovich, *AIChE J*, **51**, 2876 (2005).
7. A. S. Mukasyan, P. Epstein, P. Dinka, *Proceedings of the Combustion Institute*, **31**, 1789 (2007).
8. A. G. Merzhanov, I. P. Borovinskaya, A. E. Sytchev, SHS of nano-powders. In: Baumard J-F, editor. *Lessons in nanotechnology from traditional materials to advanced ceramics.* Dijon, France: Techna Group Srl, p. 1-27 (2005).
9. A. S. Mukasyan, A. S. Rogachev, *Prog. Energ. Comb. Sci.*, **34**, 377 (2008).
10. I. A. Filimonov, N. I. Kidin, *Comb. Explos. Shock Waves***, 41**, 639 (2005).
11. S. Ekambaram, K. C. Patil, M. Maaza, *J. Alloys Compd.*, **393**, 81 (2005).
12. K. C. Patil, S. T. Aruna, T. Mimami, "Combustion synthesis: an update", *Current Opinion in Solid State and Materials Science*, **6**, 507 (2002).
13. Y. Kitamura, N. Okinaka, T. Shibayama et al., *Powder Technology*, **176**, 93 (2007).
14. A. Sedghi, S. Baghshahi et al., *Digest J. Nanomater. Biostr.*, **6** (4), 1457 (2011).
15. Lin Cheng-Shiung, Hwang Chyi-Ching et al., *Mater. Sci. and Engineering B*, **140** 31 (2007).
16. S. Park, J. C. Lee, W. Lee et al., *J. Mater. Sci.*, **38**, 4493 (2003).
17. J. Tian, J. Wang, J. Dai, et al., *Surface & Coatings Technology*, **204**, 723 (2009).
18. G. Marci et al., V. Augugliaro, M. Lopez-Munoz et al., *J. Phys. Chem. B.*, **105**, 1026 (2001).
19. C. Shifu, Z. Wei, L. Wei et al., *Applied Surface Science*, **255**, 2478 (2008).
20. M. Cho, H. Chung et al., *Water Res.*, **38**, 1069 (2004).
21. K. Kuhn, I. Chaberny et al., *Chemosphere*, **58**, 71 (2003).
22. K. Sunada, Y. Kikuchi et al., *Environ. Sci. Technol.*, **32**, 726-728 (1998).
23. I. Ivanova, S. Kambarev, R. Popova, et al., *Biotechnology & biotechnol. eq. – special edition*, Second Balkan Confer. on Biology, 21-23 May 2010, Plovdiv; 567-570 (2010).
24. J. Sawai, T. Yoshikawa, *J. Appl. Microbiology*, **96**, 803 (2004).
25. N. Jones, B. Ray et al., *Microbiology Lett.*, **279**, 71 (2008).
26. N. Padmavathy and R. Vijayaraghavan, *Sci. Techol. Adv. Mater.*, **9**, 035004 (2008).
27. A. Shalaby, Y. Dimitriev, R. Iordanova, A. Bachvarova-Nedelcheva, Tz. Iliev, *J. Univ. Chem. Techn. Metall.*, **46** (2), 137 (2011).
28. A. Stoyanova, H. Hitkova, A. Bachvarova-Nedelcheva, R. Iordanova, N. Ivanova, M. Sredkova, *J. Univ. Chem. Techn. Metall.*, **48**, 154-161 (2013).
29. A. Stoyanova, A. Bachvarova-Nedelcheva, R. Iordanova, N. Ivanova, H. Hitkova, M. Sredkova, *Digest J. Nanomat. Biostr.*, **7**, 777 (2012).
30. A. Stoyanova, M. Sredkova, A. Bachvarova-Nedelcheva, R. Iordanova, Y. Dimitriev, H. Hitkova, Tz. Iliev, *Opt. Adv. Mater.-RC*, **4**, 2059 (2010).
31. Y. Dimitriev, Y. Ivanova, A. Staneva, L. Alexandrov, M. Mancheva, et al., *J. Univ. Chem. Techn. Metall.*, **44**, 235 (2009).
32. A. Bachvarova-Nedelcheva, R. Iordanova, A. Stoyanova, R. Gegova, Y. Dimitriev, A. Loukanov, *Central Eur. J. Chem.*, **11**, 364 (2013).
33. R. Gegova, A. Bachvarova-Nedelcheva, R. Iordanova, Y. Dimitriev, *J. Univ. Chem. Techn. Metall.*, **48**, 147-153 (2013).
34. M. Mancheva, R. Iordanova, Y. Dimitriev, *J. Alloys Compd.*, **509**, 15 (2011).
35. M. Andres-Verges, M. Martinez-Gailego, *J. Mater. Sci.*, **27**, 3756 (1992).
36. E. Yurchenko, G. Kustova, S. Bacanov, „*Vibratioanl spectroscopy of inorganic compounds*", Nauka, 1981 (in Russian).
37. A. I. Boldyrev, "*Infrared spectroscopy of minerals*", Nedra, 1976 (in Russian).
38. A. Murashkevich, A. Lavitkaya, T. Barannikova et al., *J. Appl. Spectr.*, **75**, 730 (2008).
39. B. Stefanov, N. Kaneva, G. Puma, C. Dushkin, *Colloids and Surfaces A: Physicochemical and Engineering Aspects*, **382**, 219 (2011).
40. K. Kumar, K. Porkodi, F. Rocha, *Cat. Comm.*, **9**, 82 (2008).
41. A. Bojinova, R. Kralchevska, I. Poulios, C. Dushkin, *Mater. Chem. Phys.*, **106**, 187 (2007).
42. X. Xu, J. Wang, J. Tian, et al., *Ceram. Intern.*, **37**, 2201 (2011).
43. A. Stoyanova, H. Hitkova, A. Bachvarova-Nedelcheva, R. Iordanova, N. Ivanova and M. Sredkova, *NanoScience and Nanotechnology*, **12**, 23 (2012).
44. Z. Emami-Karvani and P. Chehrazi, *African J. Microbiol. Res.*, **5**, 1368 (2011).
45. R. Rajendran, C. Balakumar, Hasabo A. Mohammed Ahammed, S. Jayakumar, et al., *Int. J. Eng. Sci. Techn.*, **2**, 202 (2010).
46. K. Hirota, M. Sugimoto, M. Kato, K. Tsukagoshi, T. Tanigawa, H. Sugimoto, *Ceramics International*, **36**, 497 (2010).
47. S.M. Gupta, M. Tripathi, *Chinese Science Bulletin*, **56**, 1639 (2011).
48. H. Hitkova, A. Stoyanova, N. Ivanova, M. Sredkova, R. Iordanova, A. Bachvarova-Nedelcheva, *J. Optoel. Biomed. Materials*, **4**, 9 (2012).

СИНТЕЗА, ХАРАКТЕРИЗИРАНЕ И СВОЙСТВА НА ПРАХОВЕ ОТ ZnO/TIO_2, ПОЛУЧЕНИ ПО МЕТОДА НА ИЗГАРЯНЕ В ГЕЛ

А.Д. Бъчварова-Неделчева[1*], Р.Д. Гегова[1], А.М. Стоянова[2], Р.С. Йорданова[1],В.Е. Копция[3], Н.К. Иванова[2], И. Санду[3]

[1]*Институт по обща и неорганична химия, Българска академия на науките, София*
[2] *Медицински университет, Плевен*
[3] *Инердисциплинарна платформа „Археоинвест“, Лаборатория за научни изследвания, Яш, Румъния*

Постъпила на 4 юли, 2013 г.; приета на 28 ноември, 2013 г.

(Резюме)

Получени са прахове от ZnO/TiO_2 със субмикронни размери по метода на изгаряне в гел. Охарактеризирани са структурата, морфологията и елементния състав чрез XRD, IR-спектроскопия, сканираща електронна микроскопия с SEM с EDX-анализ. Фотокаталитичната активност на пробите е оценена чрез разпадането на малахитово зелено и реактивно черно 5 във водни разтвори при облъчване с ултравиолетва светлина. Антибактериалните отнасяния на получените проби са изследвани в твърда среща (върху агар) спрямо Грам-негативните бактерии *Escherichia coli* ATCC 25922 и Грам- положителните *Staphylococcus aureus* ATCC 25923. Диаметърът на инхибиране е измерван за всички проби. Не са забелязани зони на инхибиране при контролните експерименти. Всички проби проявяват силна бактерицидна активност срещу двата избрани бактериални клетки.